# In Situ Kinetics of Cytochromes $c_1$ and $c_2$†

Vladimir P. Shinkarev,* Antony R. Crofts, and Colin A. Wraight

*Department of Biochemistry, University of Illinois, 156 Davenport Hall, 607 South Mathews Avenue, Urbana, Illinois 6l80l*

*Received January 26, 2006; Revised Manuscript Received April 17, 2006*

ABSTRACT: In *Rhodobacter sphaeroides* chromatophores, cytochromes (cyt) $c_1$ and $c_2$ have closely overlapping spectra, and their spectral deconvolution provides a challenging task. As a result, analyses of the kinetics of different cytochrome components of the $bc_1$ complex in purple bacteria usually report only the sum cyt $c_1$ + cyt $c_2$ kinetics. Here we used newly determined difference spectra of individual components to resolve the kinetics of cyt $c_1$ and $c_2$ in situ via a least-squares (LS) deconvolution. We found that the kinetics of cyt $c_1$ and $c_2$ are significantly different from those measured using the traditional difference wavelength (DW) approach, based on the difference in the absorbance at two different wavelengths specific for each component. In particular, with the wavelength pairs previously recommended, differences in instrumental calibration led to kinetics of flash-induced cyt $c_1$ oxidation measured with the DW method which were faster than those determined by the LS method (half-time of ∼120 $\mu$s vs half-time of ∼235 $\mu$s, in the presence of antimycin). In addition, the LS approach revealed a delay of ∼50 $\mu$s in the kinetics of cyt $c_1$ oxidation, which was masked when the DW approach was used. We attribute this delay to all processes leading to the oxidation of cyt $c_1$ after light activation of the photosynthetic reaction center, especially the dissociation of cyt $c_2$ from the reaction center. We also found that kinetics of both cyt $c_1$ and $c_2$ measured by the DW approach were significantly distorted at times longer than 1 ms, due to spectral contamination from changes in the *b* hemes. The successful spectral deconvolution of cyt $c_1$ and $c_2$, and inclusion of both cytochromes in the kinetic analysis, significantly increase the data available for mechanistic understanding of $bc_1$ turnover in situ.

The cytochrome (cyt)[1] $bc_1$ complex (ubihydroquinone: cytochrome *c* oxidoreductase) is the central enzyme of respiratory and photosynthetic electron transfer chains; it oxidizes ubiquinol and reduces cytochrome *c* and, through the coupled reactions of the Q-cycle, generates a transmembrane electrochemical gradient of protons (*1*−*5*). Due to the strong absorption of the cytochrome components, optical spectroscopic methods have played a major role in the elucidation of the $bc_1$ complex mechanism.

Chromatophores of purple bacteria suit well the study of the kinetics and thermodynamics of the $bc_1$ complex. Upon illumination, the photosynthetic reaction center (RC) reduces ubiquinone to ubiquinol and oxidizes a water-soluble cytochrome $c_2$, thereby creating the natural donor and acceptor substrates for the cytochrome $bc_1$ complex. Rapid light-induced activation of the $bc_1$ complex by its natural substrates provides a convenient way of studying the mechanism of the complex. As a result, $bc_1$ complexes from purple bacteria are important systems for studying the structure and function of the general class of $bc_1$-type complexes. However, in addition to the absorbance changes associated with the turnover of the $bc_1$ complex, activation of the $bc_1$ complex is also accompanied by absorbance changes originating from RCs and from cyt $c_2$.

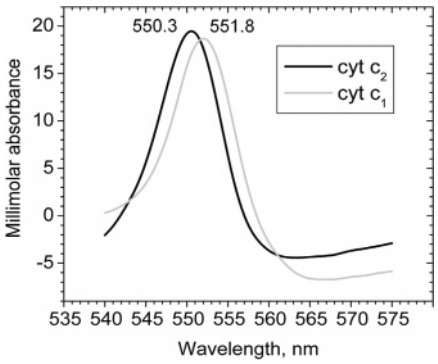


FIGURE 1: Difference spectra of cyt $c_2$ and $c_1$ in the 540−575 nm region in *Rb. sphaeroides* chromatophores (*16*). The difference spectra of cyt $c_1$ and $c_2$ have maxima at 551.8 ± 0.1 and 550.3 ± 0.1 nm, respectively (as determined by fitting the top of the band with a single Lorentzian).

Kinetic, thermodynamic, and spectroscopic properties of all the main components of cyclic electron transport have been extensively characterized in the chromatophore system (*6*−*11*). Individual components of the electron transport chain have generally been measured using the difference in absorbance at a small number (usually two) of wavelengths specific for each component, chosen to minimize the spectral overlap from other components.

Among all components of cyclic electron transport, cytochromes $c_1$ and $c_2$ have the most closely overlapped spectra (Figure 1). The initial characterization of cyt $c_1$ in

† This work was supported by National Institutes of Health Grants GM 53508 (to C.A.W. and V.P.S.) and GM 35438 (to A.R.C.).

* To whom correspondence should be addressed. Phone: (217) 333-8725. Fax: (217) 244-6615. E-mail: vshinkar@uiuc.edu.

[1] Abbreviations: CCCP, carbonyl cyanide *m*-chlorophenylhydrazone; cyt, cytochrome; DAD, 2,3,5,6-tetramethyl-*p*-phenylenediamine; DM, dodecyl maltoside; DW, difference wavelength; ISP, Rieske iron−sulfur protein; LS, least-squares; RC, photosynthetic reaction center; $Q_i$ and $Q_o$, quinone reducing and quinol oxidizing sites of the $bc_1$ complex, respectively; UHDBT, 5-undecyl-6-hydroxy-4,7-dioxobenzothiazol; $b_L$ and $b_H$, low- and high-potential hemes of cytochrome *b*, respectively.

10.1021/bi060172u CCC: $33.50 
Published on Web 06/01/2006

*Rhodobacter sphaeroides* (*12*) showed a spectrum displaced by ~2 nm to the red from that of cyt $c_2$. Meinhardt and Crofts (*10*) suggested measuring the kinetics of cyt $c_2$ at 550−554 nm and cyt $c_1$ at 552−548 nm, wavelength pairs chosen so that the extinction coefficients for the cytochrome of interest were significantly different while the extinction coefficients for the other were the same.

Using these pairs, they showed that the fast component of cyt $c_{tot}$ oxidation mostly contributed by cyt $c_2$, while the slow component mostly corresponded to cyt $c_1$. However, significant spectral overlap of all cytochromes in chromatophores, as well as the high sensitivity of the chosen wavelength couple to small shifts in the spectra (and variations in the calibration of monochromators), has prevented wide use of these wavelength pairs. Most studies report only the sum cyt $c_1$ + cyt $c_2$ (=$c_{tot}$), measured at 551−542 nm where both *c*-type cytochromes have approximately equal absorbance.

Konishi et al. (*13*) used a deconvolution procedure and the spectrum of water-soluble cyt $c_1$ to determine the kinetics of cyt $c_2$ and soluble cyt $c_1$ in mutant cells of *Rb. sphaeroides* expressing the water-soluble heme-binding domain of cyt $c_1$. However, these authors did not include other absorbing components, such as cyt *b*, in the deconvolution. Shinkarev et al. (*14*) used an extended least-squares (LS) deconvolution procedure to include all absorbing components and were able to separate the kinetics of cyt $c_1$ and cyt $c_2$. However, it has since become clear that some of the component spectra that were used were normalized to an inappropriate baseline (*15*), which, although not important for separation of the component by simple subtraction, renders them unsuitable for deconvolution. Recently, we re-determined the difference spectra of individual components in chromatophores and isolated $bc_1$ complex (*16*), and this allowed further development of the deconvolution procedure. Our original work used only 10 different wavelengths for the analysis (*14*), but it is not clear a priori how many different wavelengths need be used for good deconvolution. In addition, no comparison between the traditional difference wavelength (DW) approach and LS analysis for cyt $c_1$ and cyt $c_2$ has been provided before.

Here we use the corrected difference spectra of individual components (*16*) to determine the kinetics of cyt $c_1$ and $c_2$ in situ via LS deconvolution from kinetic traces measured at 31 different wavelengths between 540 and 570 nm. The resulting kinetics of cyt $c_1$ and $c_2$ are compared with those determined by the traditional DW approach, using the *same* data set. We found that the traditional DW analysis gives incorrect kinetics of cyt $c_1$ and $c_2$, due to significant spectral overlap of all cytochromes in chromatophores. In addition, the high sensitivity of the chosen wavelength pairs to small offsets in monochromator settings makes it necessary to calibrate the wavelength settings carefully. We conclude that LS deconvolution is an innovation that is necessary for proper measurement of the kinetics of cyt $c_1$ and $c_2$ in situ.

## MATERIALS AND METHODS

*Growth of Cells and Isolation of Chromatophores.* Cells of wild-type *Rb. sphaeroides* Ga were grown photosynthetically at 30 °C in Sistrom's medium. After cell breakage, chromatophores were isolated by differential centrifugation (*17*).

*Spectrophotometric Measurements.* Absorption spectra were measured using an Agilent 8453 diode array spectrophotometer. Kinetics of cytochromes were measured with a single-beam kinetic spectrophotometer of local design. Light pulses were provided by a xenon flash (~5 $\mu$s half-duration).

In the DW method, the redox changes of cyt $c_1$ plus cyt $c_2$ (=$c_{tot}$) were followed at 551−542 nm (*9*, *10*). Redox changes of the individual cytochromes were measured at 552−548 nm for cyt $c_1$ and at 550−554 nm for cyt $c_2$ (*10*). The kinetics of $c_1$ and $c_2$ were determined using the least-squares (LS) method, similar to that described in ref *18*, but utilizing kinetic traces measured for all wavelengths from 540 to 570 nm. The LS method used in this paper is based on the new set of spectra of all essential absorbing species in *Rb. sphaeroides* chromatophores in the 540−575 nm region (*16*).

The monochromator [Triax 180 (JobinYvon), 1200 groves/mm grating] was calibrated using Hg vapor lamp emission bands in the α-band region. The wavelength resolution was 0.3 nm, and the reproducibility was 0.06 nm. The slit width used in kinetic measurements was set at 0.5 mm to give a bandwidth of 1.8 nm.

*Least-Squares Method.* The LS method minimizes the sum of the squares of the deviations of experimentally measured values of absorbance changes from a theoretical expectation (see, e.g., refs *13*, *14*, and *18*−*20*). The LS method is based on the representation of absorbance changes at each wavelength as the sum of the absorbance changes of each individual component. Because the spectra that are used are scaled in terms of extinction coefficients and the traces that are used as input are scaled in absorbance units, the output of the LS fit is also in absorbance units.

The absorbance change at wavelength $\lambda_i$ ($i = 1, ..., L$) is the sum of the absorbance changes for each individual component $j$ ($j = 1, ..., N$) present in the system:

$$A(\lambda_i) = \sum_{j=1}^{N} A_j(\lambda_i) \tag{1}$$

In turn, it is assumed that absorbance of each *j*th component obeys the Beer−Lambert law; i.e., the optical density of a unit path length is the product of millimolar extinction coefficient $s_j$ (with units of $mM^{-1}$ $cm^{-1}$) at each wavelength and concentration $c_j$ (in mM) of each component in solution:

$$A_j(\lambda_i) = s_j(\lambda_i)\, c_j \tag{2}$$

Combining eqs 1 and 2, we have

$$A(\lambda_i,t_k) = \sum_{j}^{N} s_j(\lambda_i)\, c_j(t_k) \tag{3}$$

We assumed that only the concentrations of individual components depend on time, so $c_j = c_j(t_k)$ ($k = 1, ..., M$).

In matrix notation this can be presented as follows:

$$\mathbf{A} = \mathbf{S}\cdot\mathbf{C} + \mathbf{E} \tag{4}$$

where $\mathbf{A} = \{a_{ik}\} \equiv A(\lambda_i,t_k)$ ($i = 1, ..., L$; $k = 1, ..., M$), $\mathbf{S} = \{s_{ij}\} \equiv s_j(\lambda_i)$ ($i = 1, ..., L$; $j = 1, ..., N$), $\mathbf{C} = \{c_{jk}\} \equiv c_j(t_k)$

($j = 1, ..., N$; $k = 1, ..., M$), and $\mathbf{E} = \{e_{ik}\}$ ($i = 1, ..., L$; $k = 1, ..., M$). **E** is the error matrix, which contains the random errors.

If matrix **S** is known (i.e., spectra of individual components are known), the unknown concentrations can be found by minimizing the sum of the squares of the deviation of the experimentally measured values of absorbance changes from the theoretical one given by eq 4; i.e., it minimizes $\mathbf{EE}^T = (\mathbf{A} - \mathbf{S}\cdot\mathbf{C})(\mathbf{A} - \mathbf{S}\cdot\mathbf{C})^T$, where the superscript T indicates the transpose of a matrix. As usual, this involves setting the derivatives to zero with respect to each unknown parameter.

Matrix $\bar{\mathbf{C}}$ (below) gives the best LS estimate of unknown matrix **C** from known matrix **S** and measured matrix **A** (*21*−*23*):

$$\bar{\mathbf{C}} = (\mathbf{S}^T\mathbf{S})^{-1}\mathbf{S}^T\mathbf{A} \quad (5)$$

where the superscript T indicates the transpose of a matrix. Equation 5 is valid only when square matrix $\mathbf{S}^T\mathbf{S}$ is invertible (nonsingular).

Ordinarily, this approach gives a unique solution when the number of wavelengths is greater than the number of individual components. However, a set of wavelengths will suffice only if they discriminate effectively between the components, and the choice of wavelengths is therefore critical to success and to the resulting signal-to-noise ratio.

All calculations were performed using Matlab (The Mathworks, Inc.).

*Reagents.* Antimycin A, azolectin, gramicidin, myxothiazol, stigmatellin, DAD, PMS, CCCP, MOPS, and Tris were obtained from Sigma-Aldrich (St. Louis, MO). Inhibitors and uncouplers were dissolved in ethanol and stored at −20 °C.

## RESULTS

*Kinetics of Cyt $c_{tot}$, $c_1$, and $c_2$ in the Presence of Antimycin Alone.* In the presence of antimycin A, an inhibitor of the $Q_i$ site, the oxidation of reduced cyt *b* is inhibited, and as a result, one can expect significant amplitudes of cyt *b* reduction and, therefore, spectral interference from this component.

Figure 2 shows the flash-induced kinetics of cyt $c_1$, $c_2$, and $c_{tot}$, determined by LS deconvolution of time series measured at 31 different wavelengths from 540 to 570 nm. These kinetic traces are shown together with kinetics of cytochrome $c_{tot}$ measured at 551−542 nm (A), as well as kinetics at the wavelength pairs previously suggested for measurement of cytochromes $c_1$ and $c_2$, at 552−548 nm (B) and 550−554 nm (C), respectively (shown in gray). Here we use a time scale split into fast (<1 ms) and slow (>1 ms) ranges, to better distinguish the kinetics of the cytochromes determined by different methods. The density of points is significantly different for fast and slow time scales ($\sim 10^2$ points on the fast time scale and $\sim 10^4$ points on the longer time scale). As a result, the noise appears to be higher for the longer time scale.

The kinetics of oxidation of cyt $c_{tot}$ ($=c_1 + c_2$) measured at 551−542 nm are very similar to those determined by LS deconvolution. As described in ref *16*, the small difference in the re-reduction phase, observed at longer times, arises from spectral contamination from cyt $b_H$. However, comparison of the individual kinetics of cyt $c_1$ and $c_2$ obtained using the wavelengths suggested by Meinhardt and Crofts (*10*) with those determined by LS deconvolution indicates that there are more substantial differences in the kinetics revealed by the two methods.

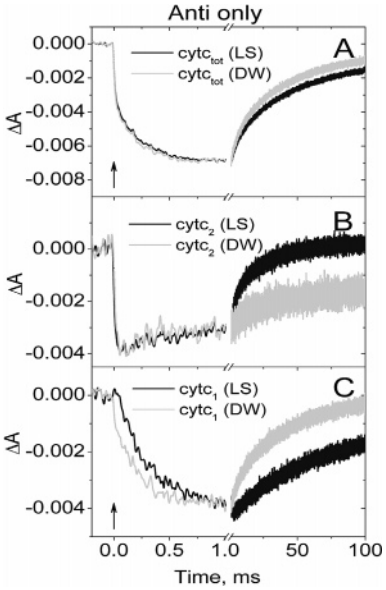


FIGURE 2: Flash-induced kinetics of cyt $c_1$, $c_2$, and $c_{tot}$ ($=c_1 + c_2$) in *Rb. sphaeroides* chromatophores in the presence of antimycin, determined by LS analysis using kinetic traces measured at 31 wavelengths from 540 to 570 nm, with a 1 nm step (black), and using the traditional DW approach (gray). In the DW approach, the kinetics of cyt $c_{tot}$, $c_1$, and $c_2$ were determined from 551 to 542 nm, from 552 to 548 nm, and from 550 to 554 nm, respectively. Chromatophores were suspended in 50 mM Tris-HCl buffer (pH 7.4) with 5 mM potassium ferrocyanide, 100 mM KCl, 100 $\mu$M DAD, 50 $\mu$M sodium ascorbate, 2 mM NaCN, 20 $\mu$M CCCP, 10 $\mu$M gramicidin, and 5 $\mu$M antimycin A. Kinetic traces at each wavelength are the average of eight traces, with 15 s between measurements, and were recorded with an instrument response time of 10 $\mu$s. In the case of the DW approach, kinetics of cyt $c_1$ and $c_2$ are normalized at 1 ms. Arrows indicate the time of the flash excitation.

For the *same* data set, the half-time of cyt $c_1$ oxidation determined by LS deconvolution is significantly longer ($\sim$235 $\mu$s) than that based on the 552−548 nm wavelength pair ($\sim$120 $\mu$s). The LS deconvolution also reveals the presence of a delay of $\sim$50 $\mu$s in the kinetics of cyt $c_1$, which is not apparent when determined via 552−548 nm. This discrepancy originates from several sources, including uncertainties in calibration of the monochromator used in previous work. In principle, the DW method should provide compensation of cyt $c_2$ changes, but it depends on a good correspondence between the recommended wavelength pair, 552−548 nm, and the spectrum returned by the monochromator used. Indeed, inspection of the corrected spectra used here (*16*) indicates that the wavelength pair of 552−548 nm gave rise to inclusion of a significant fraction of cyt $c_2$. When 552−549 or 552−549.5 nm were used instead of 552−548 nm, the kinetics observed on the fast time scale were similar to those obtained via LS deconvolution (not shown) and similar to those originally reported (*10*), but with an increased noise level due to a decrease in the amplitude of absorbance changes. This is consistent with the error range given in the earlier work (*10*) but emphasizes the sensitivity of the DW method to the precision and calibration of the wavelength setting.

There are also substantial differences in the kinetics of cyt $c_2$ and $c_1$ determined by DW and LS methods for times

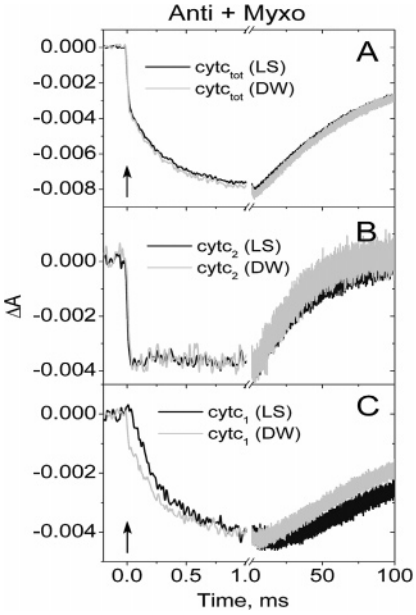


FIGURE 3: Flash-induced kinetics of cyt $c_1$, $c_2$, and $c_{tot}$ ($=c_1 + c_2$) in *Rb. sphaeroides* chromatophores in the presence of antimycin and myxothiazol, determined by LS analysis using kinetic traces measured at 31 wavelengths from 540 to 570 nm, with a 1 nm step (black), and using the traditional DW approach (gray). Special analysis methods and experimental conditions are as described in the legend of Figure 2, but in the presence of 5 $\mu$M myxothiazol. Arrows indicate the time of the flash excitation.

of >1 ms (Figure 2B), due to "contamination" from changes of the *b* heme absorbance. These cannot be avoided with minor adjustments of the wavelengths used in the DW measurements.

*Kinetics of Cyts $c_{tot}$, $c_1$, and $c_2$ in the Presence of Antimycin and Myxothiazol.* To eliminate the spectral interference from cyt *b*, we studied the kinetics of cytochromes in the presence of antimycin and myxothiazol, when the flash-induced kinetics of the *b* hemes are inhibited. Figure 3 shows the flash-induced kinetics of cyt $c_1$, $c_2$, and $c_{tot}$ ($=c_1 + c_2$) in *Rb. sphaeroides* chromatophores in the presence of both antimycin and myxothiazol. Comparison of the data in Figures 2 and 3 shows that the large difference between LS and DW approaches observed at longer times (>1 ms) in the presence of antimycin alone was due mostly to the spectral contamination from cyt *b*.

*Time-Resolved Spectra of Cytochrome Components Measured in the Presence of Antimycin.* The flash-induced kinetics of cytochromes $c_1$ and $c_2$ are significantly faster than those of cyt $b_L$ and $b_H$, which, when the Q-pool is initially oxidized, do not change their state till ~0.5 ms. Therefore, the oxidation kinetics of cyt $c_2$ and $c_1$, which occupy the range of <1 ms, can usually be measured without significant interference from cyt *b*. Furthermore, spectral interference from cyt *b* can be excluded in the presence of specific inhibitors for both $Q_i$ and $Q_o$ sites of the $bc_1$ complex (Figure 3).

Figure 4 shows time-resolved spectra measured 50 $\mu$s, 100 $\mu$s, 200 $\mu$s, 300 $\mu$s, 1 ms, and 10 ms after the flash. One can see that at times shorter than 1 ms, the observed changes mostly correspond to $P870^+$, cyt $c_1$, and cyt $c_2$. In chromatophores, the concentration of cyt $c_2$ is usually lower than the concentration of reaction centers. As a result, there is always a fraction of oxidized P870 after the flash. The contribution

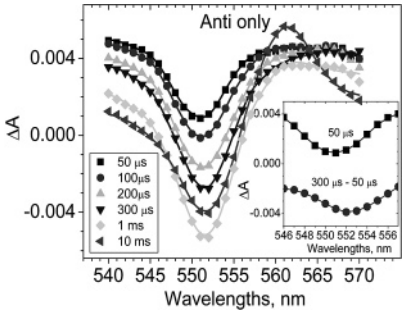


FIGURE 4: Flash-induced spectra measured in *Rb. sphaeroides* chromatophores at different times after the flash (symbols) and theoretical spectra (solid lines) calculated using LS deconvolution based on pure spectra of all individual components (P, cyts *c*, and cyts *b*). The inset shows the spectrum measured at 50 $\mu$s, mostly corresponding to cyt $c_2$, and the spectrum obtained as the difference of two traces measured at 300 and 50 $\mu$s, mostly corresponding to cyt $c_1$. Experimental conditions were as described in the legend of Figure 2.

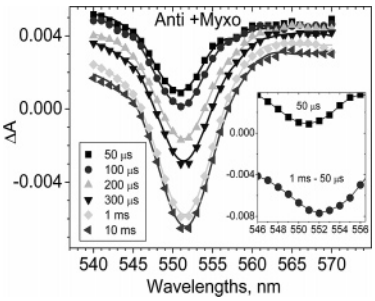


FIGURE 5: Flash-induced spectra measured in *Rb. sphaeroides* chromatophores at different times after the flash in the presence of both antimycin and myxothiazol (symbols) and theoretical spectra (solid lines) calculated using LS deconvolution based on pure spectra of all individual components (P, cyts *c*, and cyts *b*). The inset shows the spectrum measured at 50 $\mu$s, mostly corresponding to cyt $c_2$, and the spectrum obtained as the difference of two traces measured at 1 ms and 50 $\mu$s, mostly corresponding to cyt $c_1$. Conditions were as described in the legend of Figure 3.

of P870 in this spectral region is seen clearly as the time dependence of the positive absorbance near 542 nm and the skewing of the spectra of cyt *c* components.

The precise fraction of cyt $c_1$, $c_2$, and P870 in the observed spectra can be obtained only by deconvolution. The spectrum measured 50 $\mu$s after the flash has a peak at ~550.8 nm (as determined by fitting with a single Lorentzian) and is mostly due to cyt $c_2$. The approximate difference spectrum of cyt $c_1$ can be found from the difference of spectra measured at 300 and 50 $\mu$s. Indeed, the kinetic data of Figure 2 indicate that only cyt $c_2$ is oxidized at 50 $\mu$s, while cyt $c_1$ begins to be oxidized after a delay of 50 $\mu$s. Such spectra are shown in the inset of Figure 4. The minimum of the spectrum is at 552.2 nm, reflecting the increased contribution of cyt $c_1$.

At 10 ms, there is a significant increase in absorbance at 560 nm, corresponding to cyt $b_h$ reduction.

*Time-Resolved Spectra of Cytochrome Components Measured in the Presence of Antimycin and Myxothiazol.* Flash-induced changes in cyt $b_L$ and $b_H$ can be prevented when both quinone processing sites, $Q_i$ and $Q_o$, are occupied by specific inhibitors. Figure 5 shows the flash-induced spectra of chromatophores measured different lengths of time after a flash in the presence of antimycin and myxothiazol, specific inhibitors of the $Q_i$ and $Q_o$ sites, respectively, and with both *b* hemes initially oxidized. Under these conditions, P870,

cyt $c_2$, and cyt $c_1$ are the only species contributing significant spectral changes in this region and there are no significant changes in cyt *b* after the flash, even at 10 ms.

## DISCUSSION

*Kinetics of Cyts $c_1$ and $c_2$ Determined by the Traditional Difference Wavelength Method and by Least-Squares Analysis.* Cytochromes $c_1$ and $c_2$ have closely overlapped spectra, and their separate analysis provides a challenging task. Meinhardt and Crofts (*10*) attempted to separate the kinetics of cyt $c_2$ and cyt $c_1$ by the DW approach. They suggested using wavelength pairs, which have significantly different extinction coefficients for the cytochrome of interest and equal extinction coefficients for the other. However, such a DW approach, though often effective with appropriate controls, gives inadequate characterization of the kinetics of cyt $c_2$ and $c_1$ in chromatophores, as specified below.

*Cyt $c_2$.* The redox changes in cyt $c_2$ in chromatophores are usually determined from the rapid phase measured at 551−542 nm as the sum cyt $c_1$ + cyt $c_2$, or from the kinetics of P870 re-reduction. Meinhardt and Crofts (*10*) suggested that the kinetics of cyt $c_2$ be measured at 550−554 nm. The kinetics of cyt $c_2$ determined from these wavelengths for times of <1 ms are close to the kinetics determined by LS deconvolution. However, we observed a significant difference at longer times due to spectral interference from cyt $b_H$ and $b_L$. In contrast, the LS approach provides a correct description of the kinetics of cyt $c_2$ for both fast and slow time scales.

*Cyt $c_1$.* Meinhardt and Crofts (*10*) suggested that the kinetics of cyt $c_l$ be measured at 552−548 nm, assuming that the difference in the extinction coefficients for cyt $c_2$ at these wavelengths was zero, as determined by reference to the spectra they measured. However, we found significant residual differential absorbance of cyt $c_2$ at these wavelengths, leading to modification of the measured kinetics of cyt $c_1$ on the fast time scale. The extent of the discrepancy depends on the calibration of the monochromator wavelength, and this reveals a weakness of the DW approach, which can however be corrected by careful calibration. For the *same* data set, the LS deconvolution reveals a delay of ∼50 $\mu$s in the kinetics of cyt $c_1$ that was "masked" in the DW analysis due to the use of a wavelength pair that was not appropriate for the calibration that was used. As a result, the half-time of cyt $c_1$ oxidation based on the DW analysis (∼120 $\mu$s) appears to be significantly faster than that determined by the LS deconvolution (∼235 $\mu$s).

There is also a significant difference in the kinetics of cyt $c_1$ determined by DW and LS methods on slower time scales, originating from significant differential absorbance of both cyt *b* hemes at the wavelengths used. We conclude that while separation between cyt $c_1$ and $c_2$ at fast time scales can be achieved by small adjustments of the wavelength pair suggested by Meinhardt and Crofts (*10*), for example to 552−549 nm, this wavelength pair still does not accurately measure the kinetics of cyt $c_1$ for longer times (>1 ms), where interference with cyt *b* cannot be avoided.

*Delay before the Onset of Cyt $c_1$ Oxidation.* The observed delay in cyt $c_1$ oxidation reflects all processes leading to the oxidation of cyt $c_1$ after P870 photooxidation and includes the time of oxidation of cyt $c_2$ by $P870^+$, the dissociation of oxidized cyt $c_2$ from the RC, the diffusion of cyt $c_2$ to the $bc_1$ complex, and functional binding to the $bc_1$ complex. In addition, the stoichiometry requires a recycling of cyt $c_2$ to complete the oxidation of both ISP and cyt $c_1$ in the absence of stigmatellin. Thus, the delay can also be influenced by fast electron transfer from the Rieske iron−sulfur protein (ISP) to cyt $c_1$. The time of oxidation of cyt $c_2$ by $P870^+$ is ∼1 $\mu$s, for cyt $c_2$ which is already bound to the RC (*24*, *25*). The time of dissociation of cytochrome from the complex with RC depends significantly on the ionic strength of the medium (*26*, *27*) and pH (*26*−*28*), and different values from 30 $\mu$s (high-salt conditions) to 2 ms (low-salt conditions) have been reported (*26*, *27*, *29*−*33*). In our experiments, the reaction medium contained 100 mM KCl, approaching the high-ionic strength conditions used in the RC studies. The similarity of the time of delay measured here and the time of dissociation of cyt $c_2$ from the RC for a high salt concentration indicates that the delay could reflect this dissociation. However, the time for diffusion of cyt $c_2$ between the RC and nearest $bc_1$ complex, and the time of binding to the $bc_1$ complex in the formation of a functional unit, could both possibly be on the same time scale as the lag phase. Resolution of this question will therefore require further study of pH and ionic strength dependence to establish the dominant process. Nevertheless, our studies presented here show that LS deconvolution can provide unique insights into processes such as complex dissociation between different electron transfer proteins in situ.

*Kinetics of Cyt $c_1$ Oxidation.* The observed lifetime of cyt $c_1$ is clearly not the time for electron transfer between $c_2$ and $c_1$ in the $c_2$•$bc_1$ complex, which can be expected to be less than 0.1 $\mu$s (*34*). On the basis of in vitro studies (*7*, *24*−*33*, *35*, *36*; reviewed in ref *37*), the measured time of cyt $c_1$ oxidation might be assumed to arise from the diffusion of the cyt $c_2$ from the RC and formation of the complex between cyt $c_2$ and $c_1$. However, at the concentrations estimated in vivo (*7*, *38*), formation of the bimolecular complex should be at least an order of magnitude faster than the observed rate of oxidation. It is certainly possible that the unbinding of cyt $c_2$ from RC is the origin of the slow kinetics, but the in vivo kinetics have never been characterized in this way. Furthermore, because the content of cyt $c_2$ is normally substoichiometric with respect to reaction centers, completion of the high-potential reactions between RC and $bc_1$ requires multiple shuttles of cyt $c_2$, giving rise to slower phases of cyt $c_1$ oxidation. Proper characterization of the cyt $c_2$ shuttle and the different kinetic components of cyt $c_1$ oxidation will require spectral and temporal separation of $c_2$ and $c_1$, and quantitative inclusion of the binding partition for cyt $c_2$ between RC and $bc_1$ at the time of the flash. This can now be attempted with the LS analysis described here.

*Significance.* Comparison of cyt $c_1$ and $c_2$ kinetics measured by DW and LS approaches reveals that in many cases the kinetics of both cytochromes are significantly distorted in the former approach due both to incomplete separation of cyt $c_1$ and $c_2$ and to spectral interference from cyt *b*. As a result, any conclusion about mechanism drawn from DW measurements should be treated with caution, and a reevaluation of some underlying processes may be in order. Examples of issues that can be addressed with the kinetic resolution provided by the LS method include (i) discriminating between two very different models to account for why the apparent equilibrium constants in the high-potential chain

differ from those expected from redox midpoint potentials [supercomplex formation (*39*) or chromatophore heterogeneity (*40*)]; (ii) accurate measurement of electron delivery and throughput in the high- and low-potential chains, e.g., matching the kinetics of cyt $c_1$ and cyt $b_H$ during quinol oxidation at the $Q_o$ site (*41*); (iii) discrimination of $b_H$ and $b_L$ hemes in normal turnover and in reverse function via the $Q_i$ site; (iv) clarification of the effects of different inhibitors (stigmatellin and UHDBT) and separation of their effects on cyt $c_1$ and $c_2$; and (v) mechanism of exchange of electrons between the $bc_1$ complex and the reaction center facilitated by cyt $c_2$, including determination of kinetics of binding and unbinding of cyt $c_2$ and the RC in situ. More generally, the LS method provides the basis for greatly improved resolution of events in cyt $bc_1$ turnover, and the results of this paper demonstrate the essential methodology for more challenging measurements of the true kinetics and thermodynamics of the $c_1$ and $c_2$ hemes in situ.

*Limitations of the LS Analysis.* Least-squares analysis provides a natural way of deconvoluting overlapping spectral bands when the spectra of individual components are known, and no other absorbing species contribute to the observed changes. The main advantage of the LS approach is the use of the balance equations (eqs 1 and 2), which are not used in the DW approach.

In the current application of the LS method for analysis of the kinetics of cyt $c_1$ and $c_2$, we did not consider the possible dependence of the spectra of individual components on the presence of inhibitors, on the redox state of other components, on changes in the protein environment, for example, during the docking of cyt $c_2$ to the RC or cyt $c_1$, or on membrane potential. These dependencies are difficult to address properly in both LS and DW approaches. However, in many cases, these dependencies induce relatively small changes in spectra, and as a first approximation, one can ignore these effects.

*Need for a Simplified Version of LS Analysis Based on Smaller Sets of Wavelengths.* To separate the kinetics of cyt $c_1$ and $c_2$, we measured kinetic traces for all 31 wavelengths between 540 and 570 nm. While providing a very high accuracy, this approach demands significant time, making it impractical for routine experiments. From this point of view, it would be desirable to develop a simplified LS approach, based on a smaller set of wavelengths but with a quality of deconvolution similar to that based on the full set of wavelengths. The quality of deconvolution can be characterized in terms of both the difference between the original and fitted transients at each wavelength and the noise level of individual components determined for different sets of wavelengths. Such a simplified LS approach for recovering all main components of the cyclic electron transport in chromatophores from a minimal number of wavelengths requires extensive additional analysis of these parameters and will be presented elsewhere.

## ACKNOWLEDGMENT

We thank Jonathan Larson for a major contribution to instrumentation.

## REFERENCES

1. Cramer, W. A., and Knaff, D. B. (1990) *Energy Transduction in Biological Membranes*, Springer-Verlag, New York.
2. Berry, E. A., Guergova-Kuras, M., Huang, L. S., and Crofts, A. R. (2000) Structure and function of cytochrome *bc* complexes, *Annu. Rev. Biochem. 69*, 1005−1075.
3. Trumpower, B. L. (2002) A concerted, alternating sites mechanism of ubiquinol oxidation by the dimeric cytochrome $bc_1$ complex, *Biochim. Biophys. Acta 1555*, 166−173.
4. Crofts, A. R. (2004) Proton-coupled electron transfer at the $Q_o$-site of the $bc_1$ complex controls the rate of ubihydroquinone oxidation, *Biochim. Biophys. Acta 1655*, 77−92.
5. Mulkidjanian, A. Y. (2005) Ubiquinol oxidation in the cytochrome $bc_1$ complex: Reaction mechanism and prevention of short-circuiting, *Biochim. Biophys. Acta 1709*, 5−34.
6. Dutton, P. L., and Jackson, J. B. (1972) Thermodynamic and kinetic characterization of electron transfer components in situ in *Rhodopseudomonas sphaeroides* and *Rhodospirillum rubrum*, *Eur. J. Biochem. 30*, 495−510.
7. Dutton, P. L., and Prince, R. C. (1978) Reaction-center-driven cytochrome interactions, in *The Photosynthetic Bacteria* (Clayton, R. K., and Sistrom, W. S., Eds.) pp 525−570, Plenum Press, New York.
8. Bowyer, J. R., and Crofts, A. R. (1981) Light-induced red shift of the $Q_x$ absorption band of light-harvesting bacteriochlorophyll in *Rps. capsulata* and *Rps. sphaeroides*, *Arch. Biochem. Biophys. 207*, 416−426.
9. Bowyer, J. R., Meinhardt, S. W., Tierney, G. V., and Crofts, A. R. (1981) Resolved difference spectra of redox centers involved in photosynthetic electron flow in *Rhodopseudomonas capsulata* and *Rps. sphaeroides*, *Biochim. Biophys. Acta 635*, 167−186.
10. Meinhardt, S. W., and Crofts, A. R. (1982) Kinetic and thermodynamic resolution of cytochrome $c_1$ and cytochrome $c_2$ from *Rps. sphaeroides*, *FEBS Lett. 149*, 223−227.
11. Meinhardt, S. W., and Crofts, A. R. (1983) The role of cytochrome $b_{566}$ in the electron transfer chain of *Rps. sphaeroides*, *Biochim. Biophys. Acta 723*, 219−230.
12. Wood, P. M. (1980) The interrelation of the two c-type cytochromes in *Rhodopseudomonas sphaeroides* photosynthesis, *Biochem. J. 192*, 761−764.
13. Konishi, K., Vandoren, S. R., Kramer, D. M., Crofts, A. R., and Gennis, R. B. (1991) Preparation and characterization of the water-soluble heme-binding domain of cytochrome $c_1$ from the *Rhodobacter sphaeroides* $bc_1$ complex, *J. Biol. Chem. 266*, 14270−14276.
14. Shinkarev, V. P., Crofts, A. R., and Wraight, C. A. (2001) The electric field generated by photosynthetic reaction center induces rapid reversed electron transfer in the $bc_1$ complex, *Biochemistry 40*, 12584−12590.
15. Meinhardt, S. W. (1983) Electron transfer reactions of the ubiquinol:cytochrome $c_2$ oxidoreductase of *Rhodopseudomonas sphaeroides*, Ph.D. Thesis, University of Illinois, Urbana, IL.
16. Shinkarev, V. P., Crofts, A. R., and Wraight, C. A. (2006) Spectral analysis of the $bc_1$ complex components in situ: Beyond the traditional difference approach, *Biochim. Biophys. Acta 1757*, 67−77.
17. Drachev, L. A., Kaurov, B. S., Mamedov, M. D., Mulkidjanian, A. J., Semenov, A. J., Shinkarev, V. P., Skulachev, V. P., and Verkhovsky, M. I. (1989) Flash-induced electrogenic events in the photosynthetic reaction center and *bc* complex of *Rhodobacter sphaeroides* chromatophores, *Biochim. Biophys. Acta 973*, 189−197.
18. Shinkarev, V. P., Dracheva, S. M., and Drachev, A. L. (1990) The thermodynamic characteristic of four-heme cytochrome *c* in *Rhodopseudomonas viridis* reaction centers, as derived from a quantitative analysis of the difference absorption spectra in α domain, *FEBS Lett. 261*, 11−13.
19. Rich, P. R., Heathcote, P., and Moss, D. A. (1987) Kinetic-studies of electron-transfer in a hybrid system constructed from the cytochrome *bf* complex and photosystem I, *Biochim. Biophys. Acta 892*, 138−151.
20. de Wolf, F. A., Krab, K., Visschers, R. W., de Waard, J. H., and Kraayenhof, R. (1988) Studies on well-coupled Photosystem 1-enriched subchloroplast vesicles: Characteristics and reinterpretation of single-turnover cyclic electron transfer, *Biochim. Biophys. Acta 936*, 487−503.
21. Bates, D. M., and Watts, D. G. (1988) *Nonlinear Regression Analysis and Its Applications*, John Wiley & Sons Inc., New York.
22. Draper, N. R., and Smith, H. (1998) *Applied Regression Analysis*, John Wiley & Sons Inc., New York.

23. Johnson, R. A., and Wichern, D. W. (1998) *Applied Multivariate Statistical Analysis*, 4th ed., Prentice Hall, Upper Saddle River, NJ.
24. Tiede, D. M., Vashishta, A. C., and Gunner, M. R. (1993) Electron transfer kinetics and electrostatic properties of the *Rhodobacter sphaeroides* reaction center and soluble *c*-cytochromes, *Biochemistry 32*, 4515−4531.
25. Drepper, F., and Mathis, P. (1997) Structure and function of cytochrome $c_2$ in electron transfer complexes with the photosynthetic reaction center of *Rhodobacter sphaeroides*: Optical linear dichroism and EPR, *Biochemistry 36*, 1428−1440.
26. Gerencser, L., Laczko, G., and Maroti, P. (1999) Unbinding of oxidized cytochrome *c* from photosynthetic reaction center of *Rhodobacter sphaeroides* is the bottleneck of fast turnover, *Biochemistry 38*, 16866−16875.
27. Larson, J. W. (2000) Cytochrome *c* oxidation by the bacterial photosynthetic reaction center from *Rhodobacter sphaeroides*, Ph.D. Thesis, University of Illinois, Urbana, IL.
28. Witthuhn, V. C., Gao, J., Hong, S., Halls, S., Rott, M. A., Wraight, C. A., Crofts, A. R., and Donohue, T. J. (1997) Reactions of isocytochrome $c_2$ in the photosynthetic electron transfer chain of *Rhodobacter sphaeroides*, *Biochemistry 36*, 903−911.
29. Moser, C. C., and Dutton, P. L. (1988) Cytochrome *c* and $c_2$ binding dynamics and electron transfer with photosynthetic reaction center protein and other integral membrane redox proteins, *Biochemistry 27*, 2450−2461.
30. Wachtveitl, J., Farchaus, J. W., Mathis, P., and Oesterhelt, D. (1993) Tyrosine 162 of the photosynthetic reaction center L subunit plays a critical role in the cytochrome $c_2$ mediated rereduction of the photooxidized bacteriochlorophyll dimer in *Rhodobacter sphaeroides*. 2. Quantitative kinetic analysis, *Biochemistry 32*, 10894−10904.
31. Drepper, F., and Mathis, P. (1997) Structure and function of cytochrome $c_2$ in electron transfer complexes with the photosynthetic reaction center of *Rhodobacter sphaeroides*: Optical linear dichroism and EPR, *Biochemistry 36*, 1428−1440.
32. Drepper, F., Dorlet, P., and Mathis, P. (1997) Cross-linked electron transfer complex between cytochrome $c_2$ and the photosynthetic reaction center of *Rhodobacter sphaeroides*, *Biochemistry 36*, 1418−1427.
33. Graige, M. S., Feher, G., and Okamura, M. Y. (1998) Conformational gating of the electron transfer reaction $Q_A^- Q_B \rightarrow Q_A Q_B^-$ in bacterial reaction centers of *Rhodobacter sphaeroides* determined by a driving force assay, *Proc. Natl. Acad. Sci. U.S.A. 95*, 11679−11684.
34. Moser, C. C., Page, C. C., Farid, R., and Dutton, P. L. (1995) Biological electron transfer, *J. Bioenerg. Biomembr. 27*, 263−274.
35. Overfield, R. E., Wraight, C. A., and Devault, D. (1979) Microsecond photooxidation kinetics of cytochrome $c_2$ from *Rhodopseudomonas sphaeroides*: In vivo and solution studies, *FEBS Lett. 105*, 137−142.
36. Larson, J. W., and Wraight, C. A. (2000) Preferential binding of equine ferricytochrome *c* to the bacterial photosynthetic reaction center from *Rhodobacter sphaeroides*, *Biochemistry 39*, 14822−14830.
37. Axelrod, H. L., and Okamura, M. Y. (2005) The structure and function of the cytochrome $c_2$: Reaction center electron transfer complex from *Rhodobacter sphaeroides*, *Photosynth. Res. 85*, 101−114.
38. Crofts, A. R., Meinhardt, S. W., Jones, K. R., and Snozzi, M. (1983) The role of the quinone pool in the cyclic electron-transfer chain on *Rhodopseudomonas sphaeroides*: A modified Q-cycle mechanism, *Biochim. Biophys. Acta 723*, 202−218.
39. Joliot, P., Vermeglio, A., and Joliot, A. (1989) Evidence for supercomplexes between reaction centers, cytochrome $c_2$ and cytochrome $bc_1$ complex in *Rhodobacter sphaeroides* whole cells, *Biochim. Biophys. Acta 975*, 336−345.
40. Crofts, A. R., Guergova-Kuras, M., and Hong, S. (1998) Chromatophore heterogeneity explains phenomena seen in *Rhodobacter sphaeroides* previously attributed to supercomplexes, *Photosynth. Res. 55*, 357−362.
41. Crofts, A. R., Shinkarev, V. P., Kolling, D. R. J., and Hong, S. J. (2003) The modified Q-cycle explains the apparent mismatch between the kinetics of reduction of cytochromes $c_1$ and $b_H$ in the $bc_1$ complex, *J. Biol. Chem. 278*, 36191−36201.

BI060172U